LiDAR Remote Sensing Data Collection: Yamhill River, Oregon

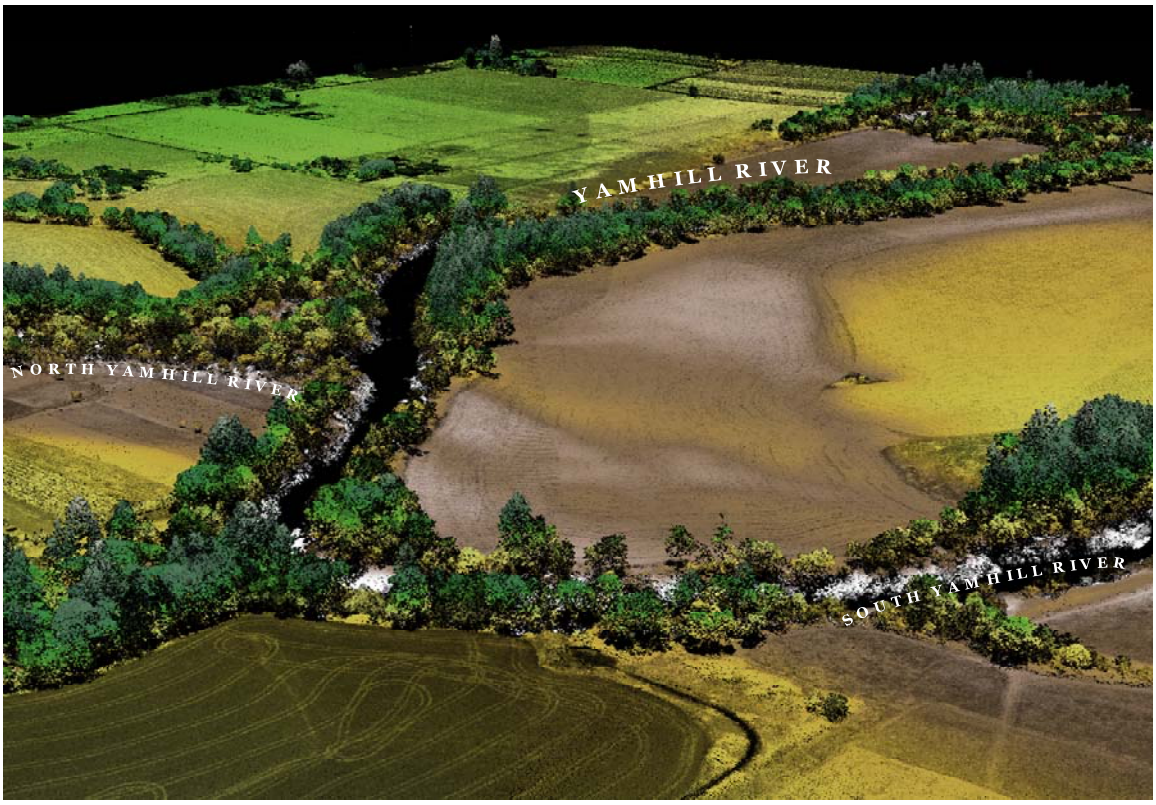

LiDAR Laser Points with Intensity Values Showing Confluence of Yamhill, North Yamhill, and South Yamhill Rivers

Submitted to:
Daniel Turner
Oregon Department of
Environmental Quality
811 SW 6th Avenue
Portland, Oregon 97204

Submitted by:
Watershed Sciences
4605 NE Fremont, Suite 211
Portland, Oregon 97213

February, 2006

Table of Contents

LIGHT DETECTION AND RANGING (LIDAR) **4**

OVERVIEW 4

TECHNICAL APPROACH **7**

Data Collection *7*

DATA PROCESSING 11

Coordinate System and Units *11*

TerraScan Processing *11*

QUALITY ASSURANCE AND CONTROL 19

DELIVERABLES **19**

SELECTED IMAGES **20**

Figures

Figure 1. 5-meter deep cross-section of laser points showing laser penetration of riparian vegetation 4
Figure 2. 10-meter deep cross-section of laser points showing laser penetration of dense vegetation 5
Figure 3. 10-meter deep cross-section of laser points showing channel obscured by vegetation. 5
Figure 4. Full extent of Study Area covering ~29,200 acres. 6
Figure 5. GPS Monument and Ground Survey Points. 9
Figure 6. Processing Bins – 141 Total Bins; approximately 1 km x 1 km each 12
Figure 7. Highest Hit vegetation model, **0.5-meter** resolution 14
Figure 8. 5x5 vegetation model, **1-meter** resolution 15
Figure 9. Vegetation Height grid, **1-meter** resolution 16
Figure 10. LiDAR-derived streams shown with vegetation height grid. 17
Figure 11. Point Divergence Statistics 18
Figure 12. Point cloud of all points with intensity values, in upper portion of study area 20
Figure 13. **0.5-meter** resolution bare ground surface, in upper portion of study area. 21
Figure 14. Point cloud of all points with intensity values, at confluence of Deer Creek 22
Figure 15. **0.5-meter** resolution bare ground surface, at confluence of Deer Creek 23
Figure 16. Point cloud of all points with intensity values, at confluence of Salt Creek 24
Figure 17. **0.5-meter** resolution bare ground surface, at confluence of Salt Creek 25
Figure 18. Point cloud of all points with intensity values, alternate view of confluence of Salt Creek 26
Figure 19. **0.5-meter** resolution bare ground surface, alternate view of confluence of Salt Creek 27
Figure 20. Point cloud of all points with intensity values, near McMinnville Airport 28
Figure 21. **0.5-meter** resolution bare ground surface, near McMinnville Airport 29

Tables

Table 1. Base Station Surveyed Coordinates / First Order NGS Monument 8
Table 2. Absolute Accuracy – Divergence between laser points and RTK survey points. 17
Table 3. LiDAR accuracy is a combination of several sources of error. 18

Light Detection and Ranging (LiDAR)

Overview

Watershed Sciences, Inc. (WS) collected Light Detection and Ranging (LiDAR) data for the Oregon Department of Environmental Quality on October 12, 2005. The survey area covers the Yamhill River and approximately ~ 20 RM of the North Fork Yamhill River. The initial study area encompassed ~20,177 acres; however, the final delivered study area covers ~29,200 acres, due to buffering and flight plan optimization.

Laser points were collected over the study area using an Optech ALTM 3100 LiDAR system set to acquire points at an average spacing of >7 points per square meter. The system also recorded individual return intensities (per laser return) that are used to create images of surface reflectivity.

Figure 1. 5-meter deep cross-section of laser points showing laser penetration of riparian vegetation at right; plan view of intensity values shown at left.

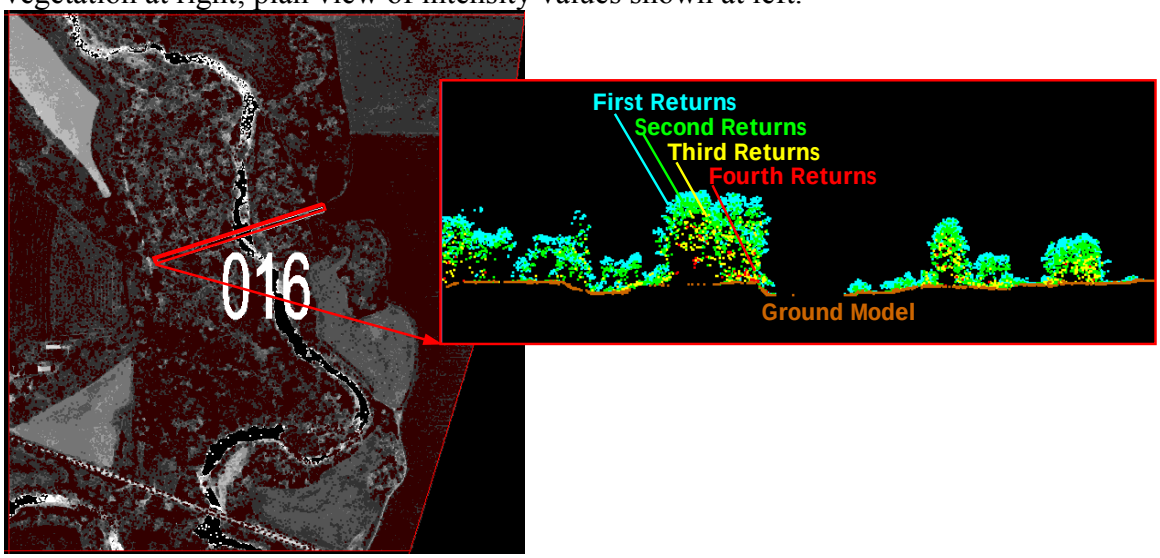

Two differential GPS units were deployed to collect 1hz static data. Kinematic solutions for the onboard GPS were combined with aircraft attitude data using PosPac 4.2. Points were computed per flight line using the REALM Survey Suite v3.5.2. Microstation V8 and TerraScan were used to import the points into bins, remove pits and birds, and compute the bare earth model. TerraModeler was then used to create TINs and output ARCINFO ASCII lattice models, which were then imported into ArcMap to render 1-meter and 0.5-meter mosaics of vegetation surfaces and ground models.

Figure 2. 10-meter deep cross-section of laser points showing laser penetration of dense vegetation at right; plan view of TIN of ground model points shown at left.

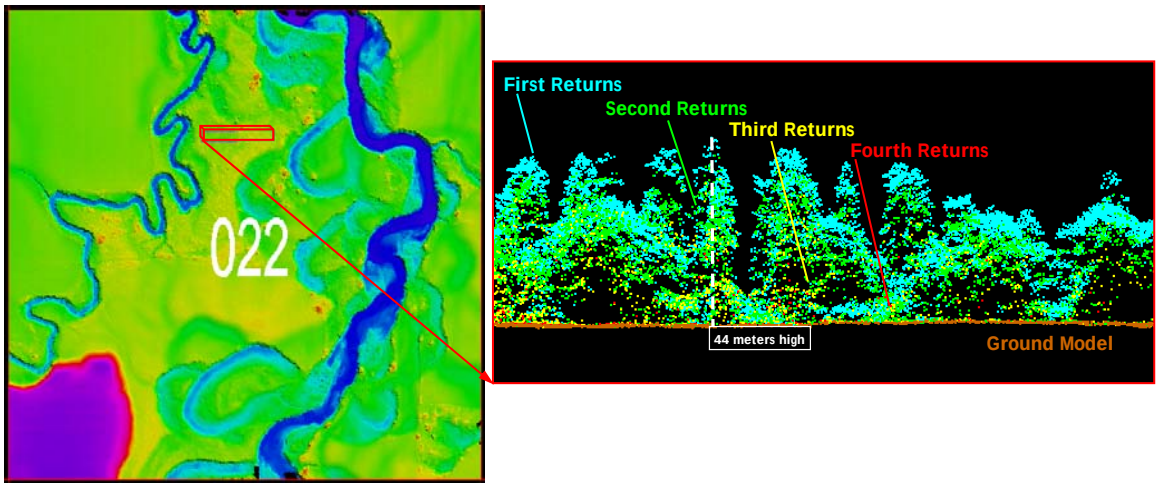

Figure 3. 10-meter deep cross-section of laser points showing channel obscured by vegetation overhang at right; plan view of TIN of ground model points shown at left.

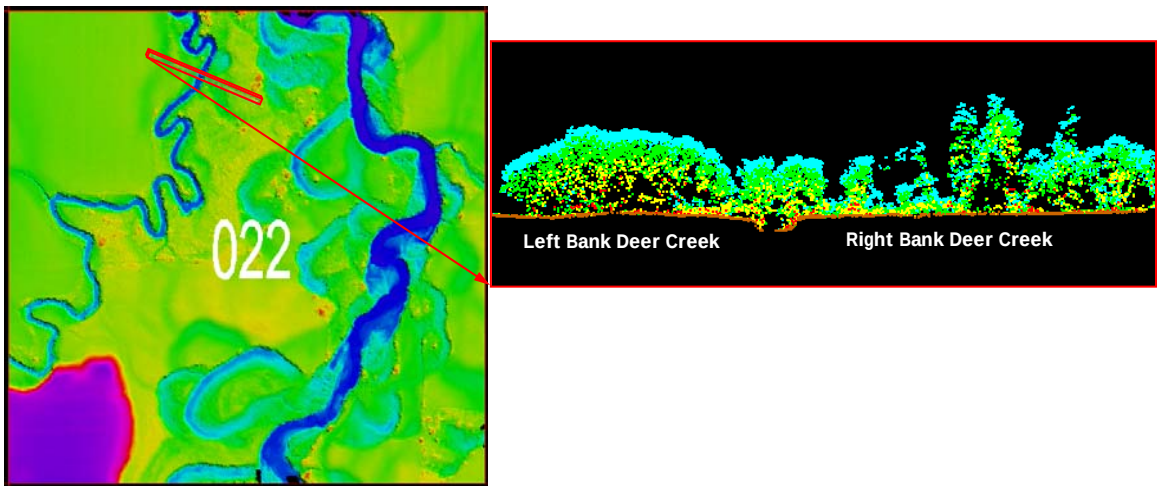

Figure 4. Full extent of Study Area covering ~29,200 acres, shown here as **1-meter** bare ground model with **10-meter** digital elevation model (DEM) in background.

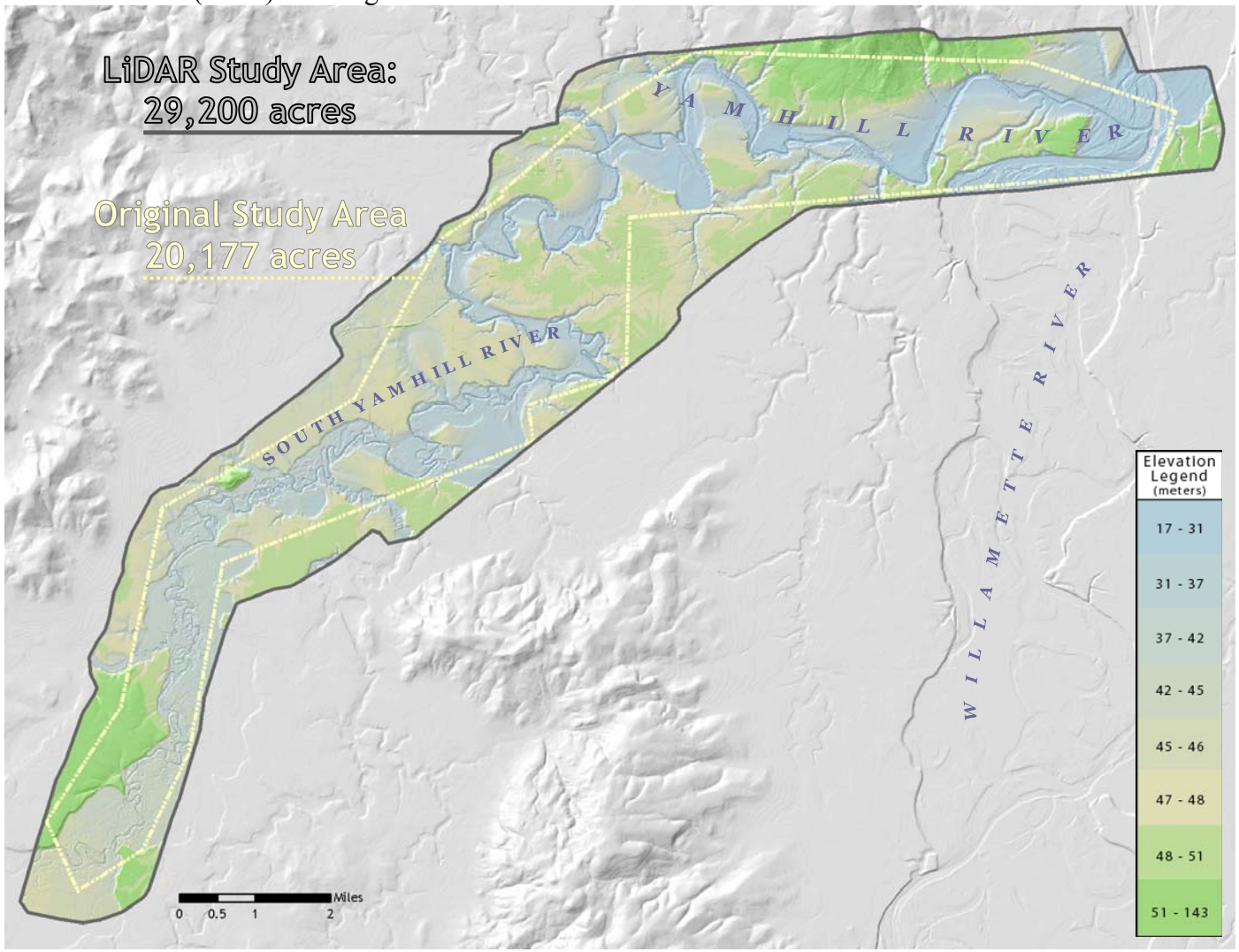

Laser point absolute accuracy is largely a function of internal consistency and laser noise:

- **Absolute Accuracy**: This is the comparison of laser points to real time kinematic (RTK) ground level survey data. A total of 577 RTK GPS measurements were compared to ground laser points collected for comparison with the LiDAR point data. The deviation RMSE and standard deviation are both 0.041 meters, with a median (50th percentile) absolute deviation of 0.033 meters and a 95th percentile of 0.071 meters.

- **Internal Consistency**: Internal consistency refers to the ability to place a laser point in the same location over multiple flight lines, GPS conditions and aircraft attitudes. The data were analyzed for internal consistency between opposing and orthogonal flight lines and passed divergence test requirements of less than 0.15 meters per any one overlapping flight line.

- **Laser Noise**: For any given target, laser noise is the breadth of the data cloud per laser return (i.e., last, first, etc.). Lower intensity surfaces (roads, rooftops, still/calm water) will experience higher laser noise. The laser noise range for this mission varies between 0.040 - 0.070 meters.

Technical Approach

Data Collection

Our LiDAR system is mounted in the belly of a Cessna Caravan 208. Quality control (QC) pre-mission flights were performed based on manufacturer's specifications prior to the survey. The QC flight was conducted at the Ashland Airport using known surveyed control points. The positional accuracy of the LiDAR (x, y, z) returns are checked against these known locations to verify the calibration and to report base accuracy.

The Optech 3100 system was set to a 71kHz laser repetition rate and flown at 1,100 meters above ground level (AGL), capturing a 30° scan width (15° from NADIR). These settings yielded points with an average spacing of >7 per square meter, with an average spot spacing of 32cm. The entire area was surveyed with opposing flight line overlap of 50% to reduce laser shadowing and increase surface laser painting. The system allows up to four range measurements per pulse, and all were processed for the output datasets. The data stream from the IMU was stored independently during the flight, and was differentially corrected and integrated with LiDAR pulse data during post processing. Throughout the survey, a dual frequency DGPS base station recorded fast static (1 Hz) data. The station was located centrally in the study area, at McMinnville Municipal Airport, (Oregon).

Data Acquisition Specifications

LiDAR Data Acquisition Feature	***Specification***
Laser Pulse Repetition Frequency	71 kHz
Laser Pulse Repetition Rate	≤71,000 pulses/sec
Operating Altitude	1,100 m AGL
Scan Frequency	37 Hz
Scan Angle	30° ($+15^o$ to -15° from Nadir)
Scan Pattern	Sawtooth
Laser Footprint Diameter on Ground (at 1,100 m AGL)	30-33 cm
Number of Returns Collected Per Laser Pulse	4
Multi-Swath Pulse Density	≥7 pulse/m^2
Intensity Range	8 bits
Minimum Resolvable Distance Between Returns	2.5 cm
Swath Width	715 m
Adjacent Swath Overlap (Side-Lap)	≥50%
Laser Spot Spacing (Cross Track = Along Track)	Single Swath: ≤0.73 m (≥2 pts/m^2) Multi Swath: ≤0.36 m (≥7 pts/m^2)
Vertical RMSE of LiDAR Survey	0.041 m
Number of GPS Base Stations Used	1
Maximum Distance From Airborne to Ground GPS	17 km (11 miles)
GPS PDOP During Acquisition	≤3.5
GPS Satellite Constellation During Acquisition	≥6
RTK Quality Control Data Points Collected	577
RTK Data RMSE	≤2.0 cm

A total of 577 quality control real-time kinematic (RTK) GPS data points were collected within the project area using a ground based DGPS station. Data collected were then compared to the processed LiDAR data to ensure accuracies across the project area.

Table 1. Base Station Surveyed Coordinates

Point ID	***NAD83NAVD88***		
	Latitude (North)	***Longitude (West)***	***Ellipsoid Height (m)***
YAMHILL 1 (OPUS corrected)	43°11'25.17489"	123°08'16.27104"	26.369

NOTE: Prior to processing, YAMHILL 1 position information was corrected using an Online Positioning User Service (OPUS) solution provided by the National Geodetic Survey (NGS). The LiDAR and RTK data were processed based on these corrected coordinates.

Figure 5. GPS Monument and Ground Survey Points. **(A)** An OPUS-corrected monument (YAMHILL 1) was used to survey fast static (1 Hz) data during the LiDAR survey.

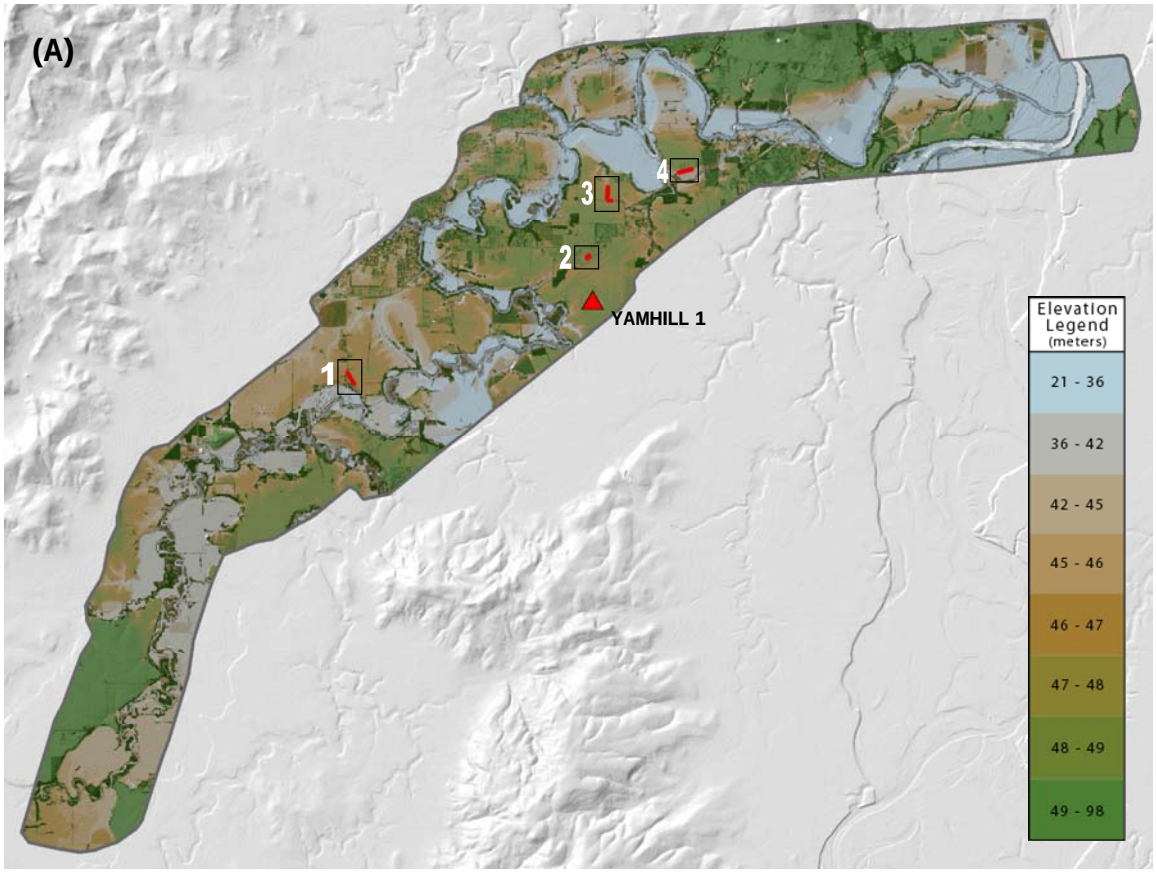

(B) A total of 577 ground survey points (RTK) were collected throughout the study area. These RTK points were used to assess data quality and accuracy. (Shown here over highest hit **1-meter** DEM with transparent DOQs).

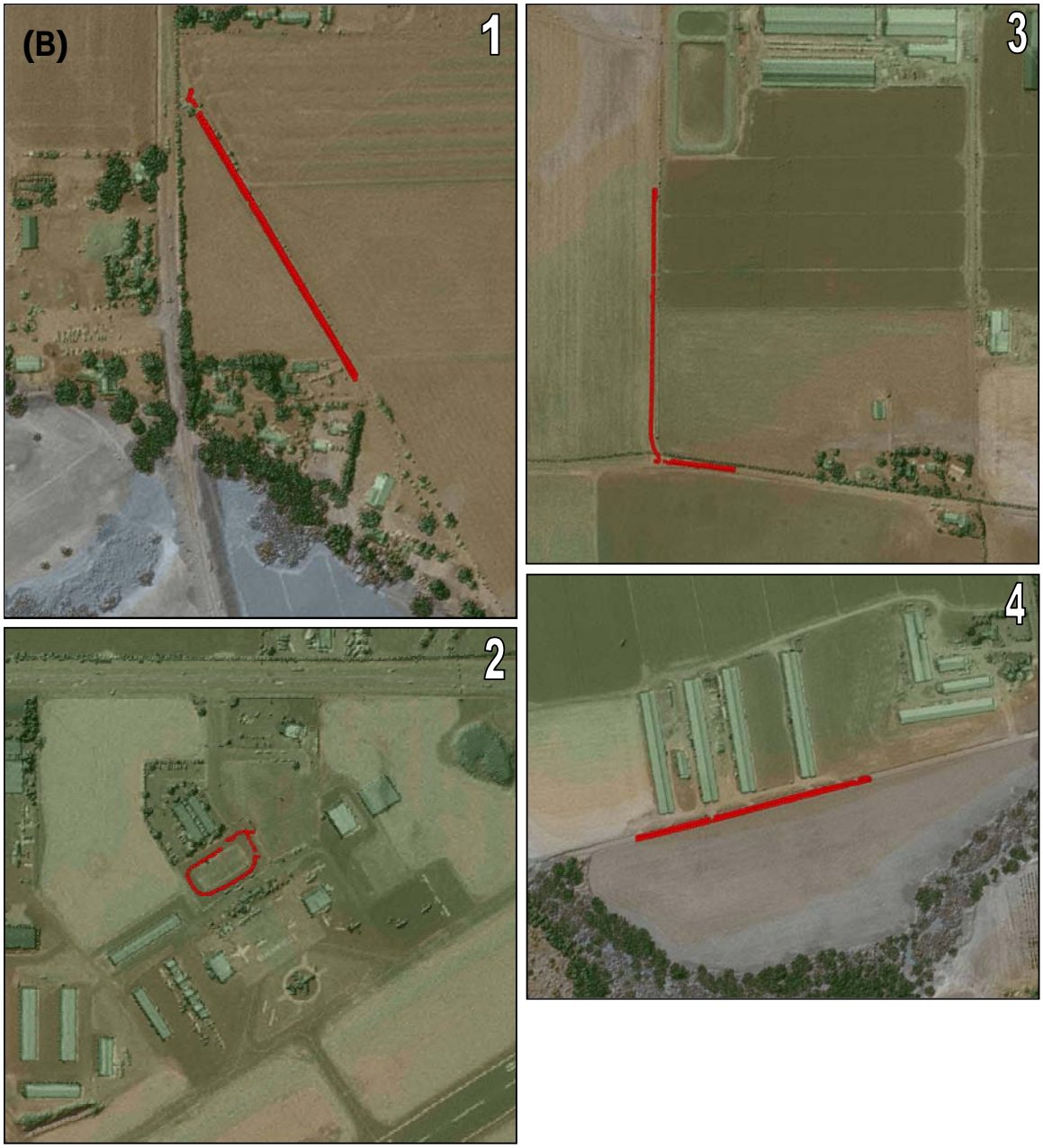

Data Processing

Coordinate System and Units

All data and imagery are developed as:

UTM 10 NAD83, NAVD88, Geoid03 Units: Meters

Laser point return coordinates were computed using the REALM software suite based on independent data from the LiDAR system (pulse time, scan angle), IMU (aircraft attitude), and aircraft position (differentially corrected and optimized using the DGPS base station data). The inertial measurement data were used to calculate the kinematic corrections for the aircraft trajectories using PosPAC v4.2. Flight lines and LiDAR data were reviewed to ensure complete coverage of the study area and positional accuracy of the laser points.

TerraScan Processing

To facilitate laser point processing, the first step is to create bins (polygons) that divide the data set into manageable sizes. The entire buffered study area was divided into 141 individual bins, approximately 1 km^2 each (see figure, below).

Laser point returns (first and last) are assigned an associated (x, y, z) coordinate, along with unique intensity values. The raw LiDAR points are filtered for noise, pits and birds by screening for absolute elevation limits, isolated points and height above ground. These data have passed initial screening and are deemed accurate.

The TerraScan software suite (Soinenen, 2004) is designed specifically for developing a standard bare earth model to remove buildings, vegetation, and other features. The high point density and multiple returns result in uncomplicated identification of vegetated and obscured areas using first and last returns. The processing sequence begins by removing all points that are not "near" the earth based on evaluation of the multi-return layers. The resulting bare earth (ground) model is visually inspected and additional ground modeling is performed in site specific areas (over a 50 meter radius) to improve ground detail. This is only done in areas with known ground modeling deficiencies, such as: bedrock outcrops, cliffs, deeply incised stream banks, and dense vegetation.

No weeding or superfluous point removal was performed. The intent of a LiDAR survey is to accurately place points on targets, not remove points. If laser noise is low and internally consistent, aside from pits and birds, it is assumed that the remaining laser returns are from targets within the survey area.

Figure 6. Processing Bins – 141 Total Bins; approximately 1 km x 1 km each, shown over highest hit **1-meter** DEM with hillshade.

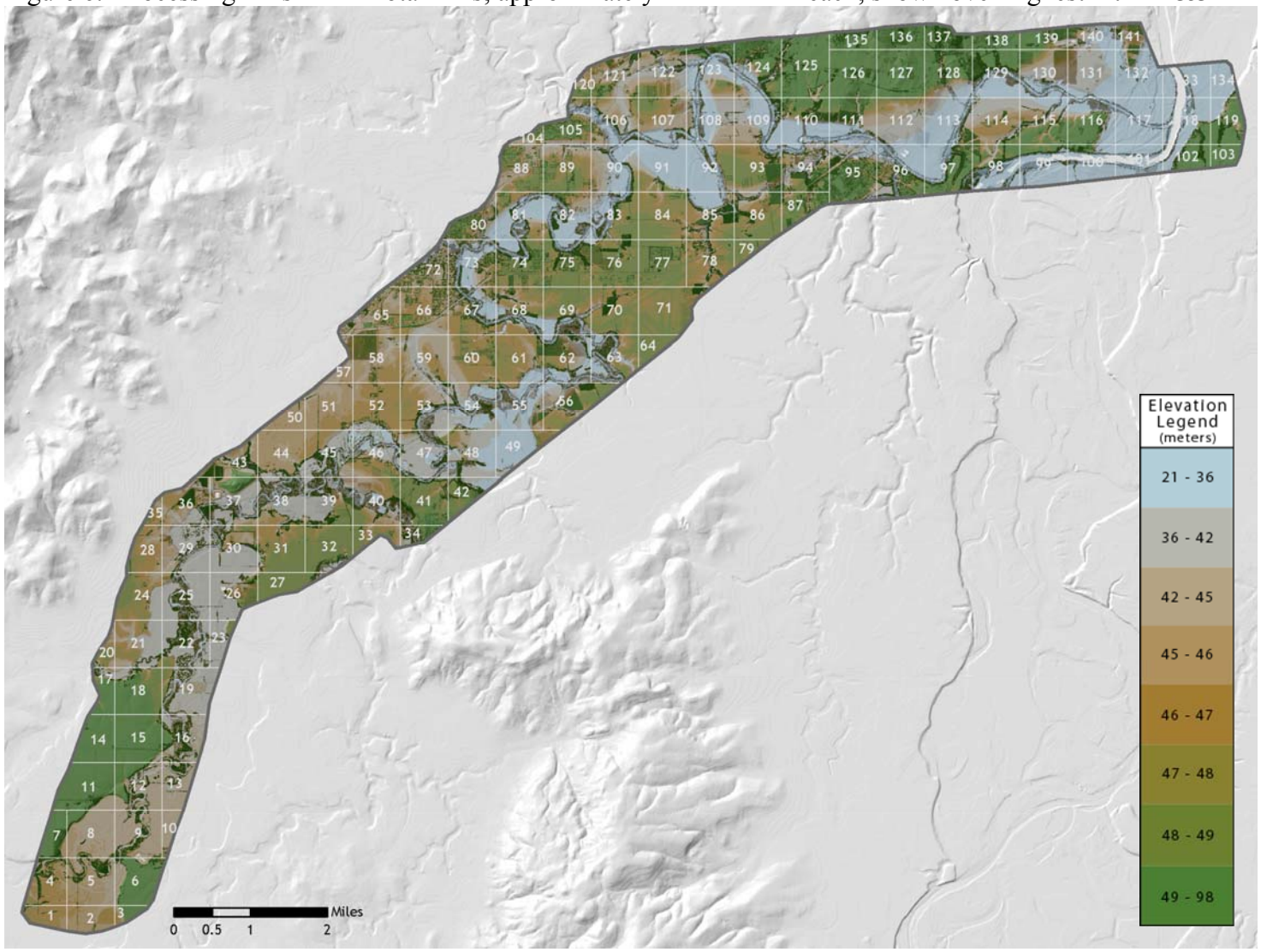

Two vegetation surface models, the 'highest hit' and the '5x5', were employed to provide greater flexibility for use. The 'highest hit' vegetation surface model is developed using all (first through fourth) accurate laser returns, using an algorithm that selects the highest laser point in a defined grid cell (in this case 0.5m) for surface creation. This results in a dataset comprised of the highest laser hits, i.e., rooftops and vegetation surfaces. This surface presents a better representation of *surface texture and variability*, which can be useful for target (e.g. vegetation type) identification.

The '5x5' vegetation model, performed using Fusion v.1.7 deforestation algorithms (Haugerud and Harding, 2001; Andersen et al. 2003; McGaughey and Carson, 2003; McGaughey, in progress[1]) also uses all (first through fourth) laser returns, but employs a moving window neighborhood function to create a 1-meter resolution model of vegetation and landscape features. This surface provides more accurate *locations* of surface elevation values.

Using the difference between the 1-meter 5x5 vegetation surface model and the 1-meter bare earth (ground) model, we have created a vegetation height dataset (ESRI GRID format). Null values in this dataset represent areas of insufficient information, such as on steep slopes where interpolation in either input GRID is not of sufficient resolution.

The following images demonstrate the differences between the three vegetation datasets.

[1] McGaughey, *in progress*. Fusion v. 1.7 development and testing.

Figure 7. Highest Hit vegetation model, **0.5-meter** resolution; this model provides better surface textures for target characterization.

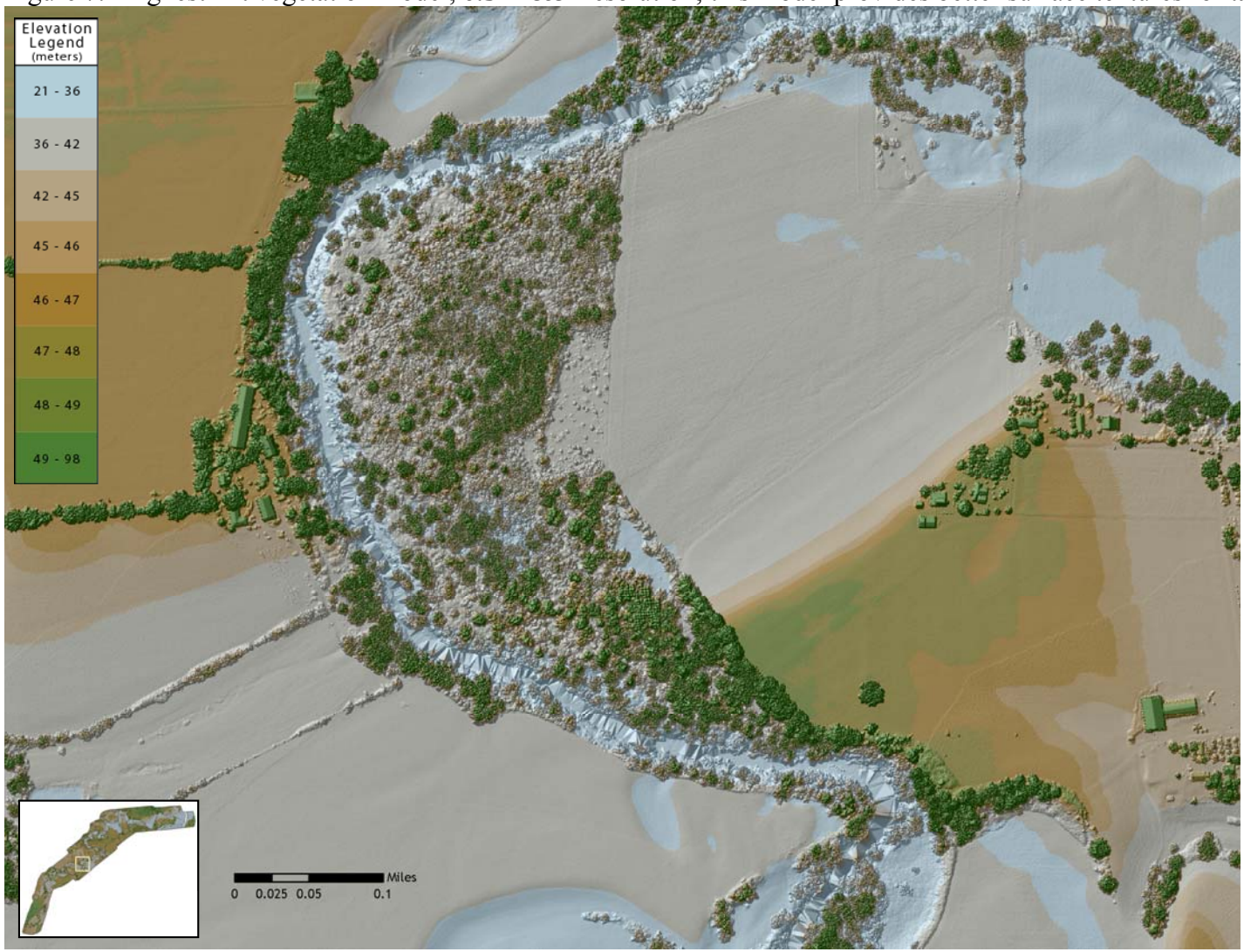

Figure 8. 5x5 vegetation model, **1-meter** resolution; this model provides more accurate locations of target elevations.

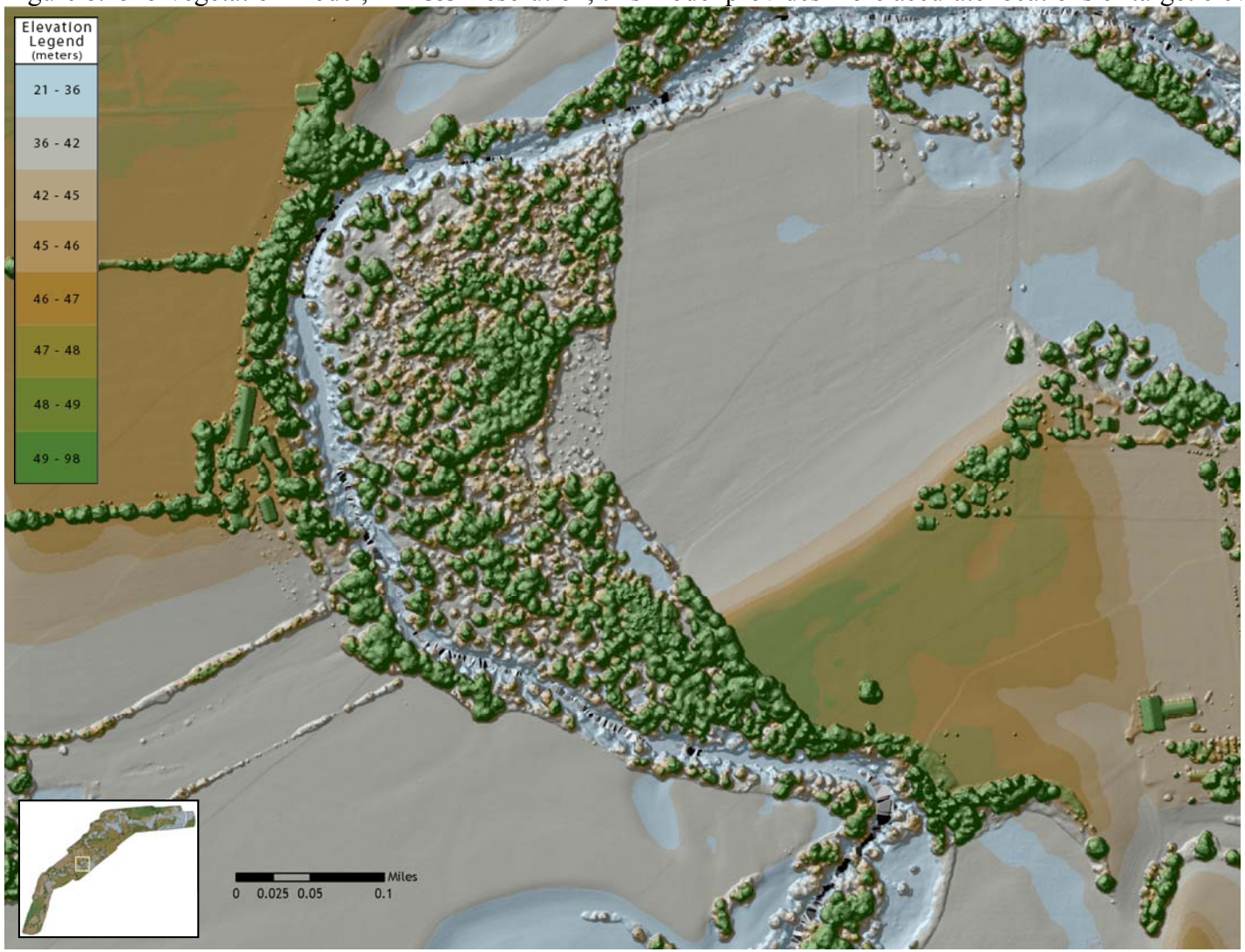

Figure 9. Vegetation Height grid, **1-meter** resolution; this GRID provides absolute heights for targets.

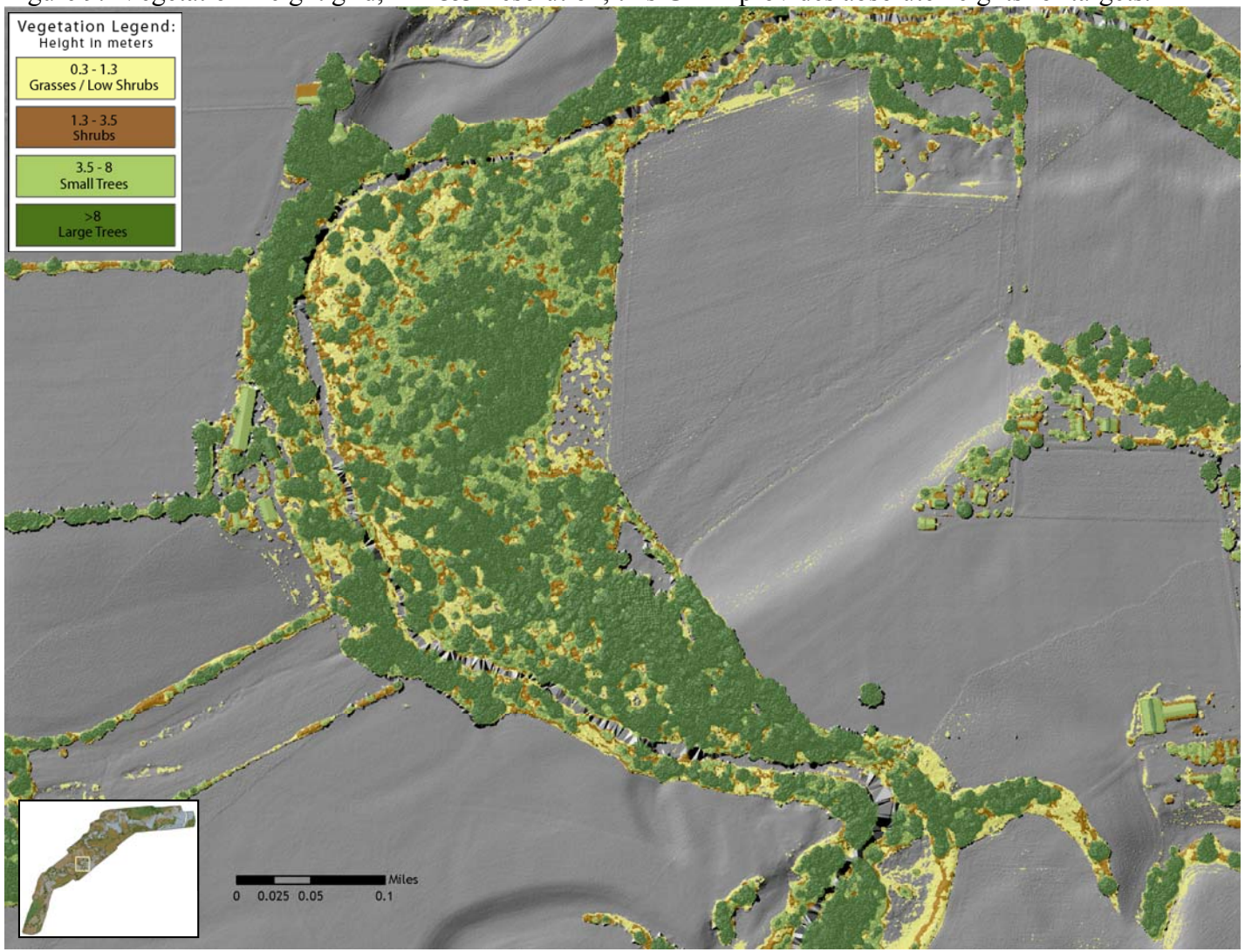

Stream Layer

The Watershed Delineation Tool WSDT V.1 (provided in the deliverables) was used to create a stream layer for the study area. This delineation is derived from the 1-meter bare earth LiDAR grid, using ~15 1 km^2 bins at a time with a 5,000 cell threshold.

Figure 10. LiDAR-derived streams shown with vegetation height grid.

Statement of Accuracy

Table 2. Absolute Accuracy – Divergence between laser points and RTK survey points.

Standard Deviation:	0.041 m	5th Percentile:	0.0048 m
RMSE:	0.041 m	25th Percentile:	0.017 m
n:	577	50th Percentile:	0.033 m
Minimum Δz:	-0.129	75th Percentile:	0.049 m
Maximum Δz:	0.113	95th Percentile:	0.071 m
Average Magnitude:	0.001 m		

Figure 11. Point Divergence Statistics
(A) Ground survey point deviation from laser points
(B) Absolute deviation from laser points, with percentile statistics

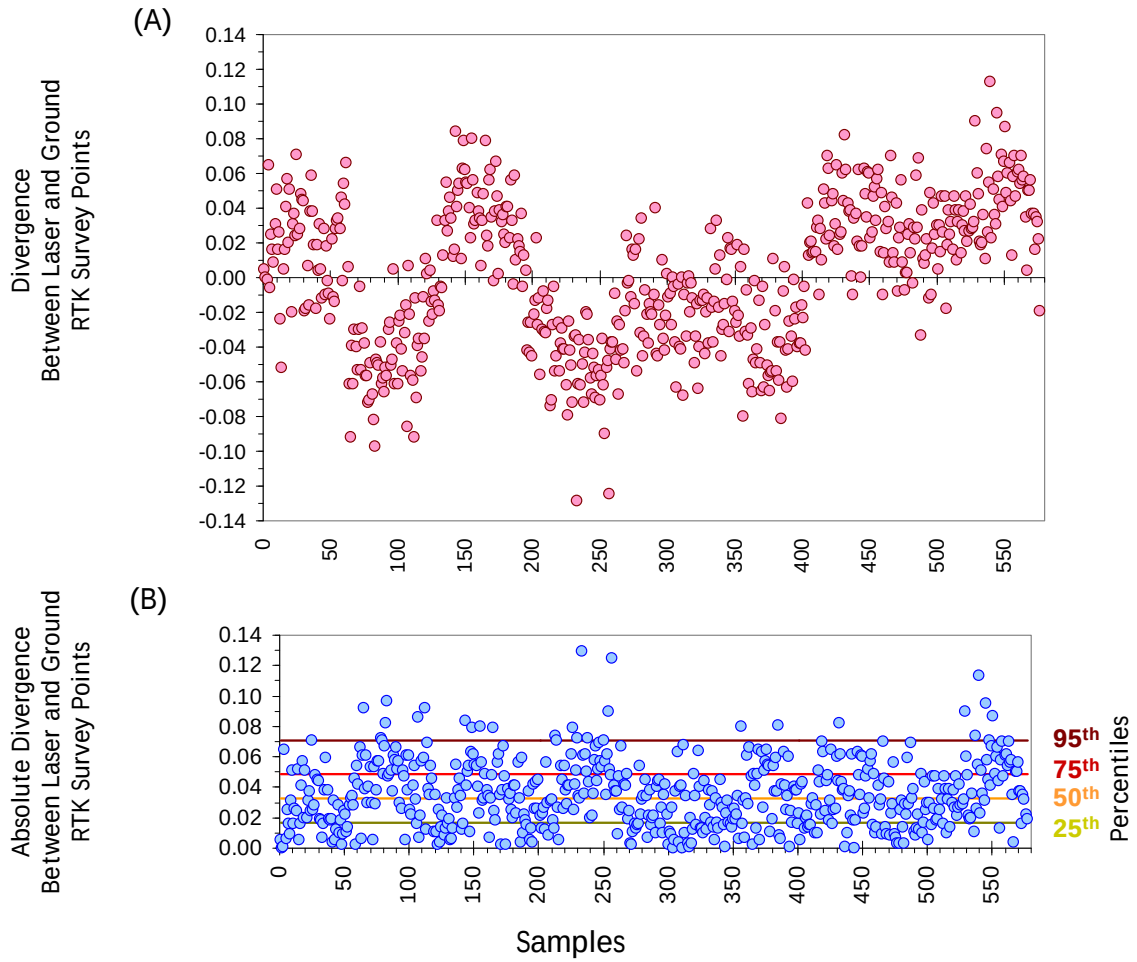

Table 3. LiDAR accuracy is a combination of several sources of error. These sources of error are cumulative. Some error sources that are biased and act in a patterned displacement can be resolved in post processing.

Type of Error	Source	Post Processing Solution	Effect
GPS (Static/Kinematic)	Long Base Lines	None	
	Poor Satellite Constellation	None	
	Poor Antenna Visibility	Reduce Visibility Mask	Slight
Internal Consistency	Poor System Calibration	Recalibration IMU and sensor offsets/settings	Large
	Inaccurate System	None	
Laser Noise	Poor Laser Timing	None	
	Poor Laser Reception	None	

Quality Assurance and Control

Quality assurance and control is built into the overall methodology. The data collection was monitored using the diagnostic features of the system during the flight. The precise navigation system and 50% side over-lap during acquisition is designed to eliminate missing coverage and ensure laser painting of multiple sides of surfaces. Over areas with significant topographic relief, additional lines were flown to ensure complete and consistent overlap. The quality of the GPS signal (or PDOP) was recorded throughout the flight and only PDOP values less than 3.5 were accepted.

All of the data are delivered on external drive, along with this report.

Deliverables

Data Report

Points

- ASCII: all returns
  (Fields are: class, easting, northing, elevation, intensity)

Rasters

- **Grids**

  Bare Earth:
  0.5 meter resolution mosaics (three grids)
  1.0 meter resolution mosaic

  Vegetation:
  -Highest Hit Model
  0.5 meter resolution mosaics (three grids)

  -5x5 Model
  1.0 meter resolution mosaic

- **Intensity Images**
  GEOTIFF images per bin

Coverages

- **Bins**
- **LiDAR-Derived Streams**

Selected Images

The following image pairs show examples of vegetation coverage and underlying channel morphology in the South Yamhill River and two of its tributaries. Each pair includes a point cloud followed by a bare ground model of the **same scene**.

Figure 12. Point cloud of all points with intensity values, in upper portion of study area (bins 9-10 and 12-13). Shown in oblique view using 3-D modeling software.

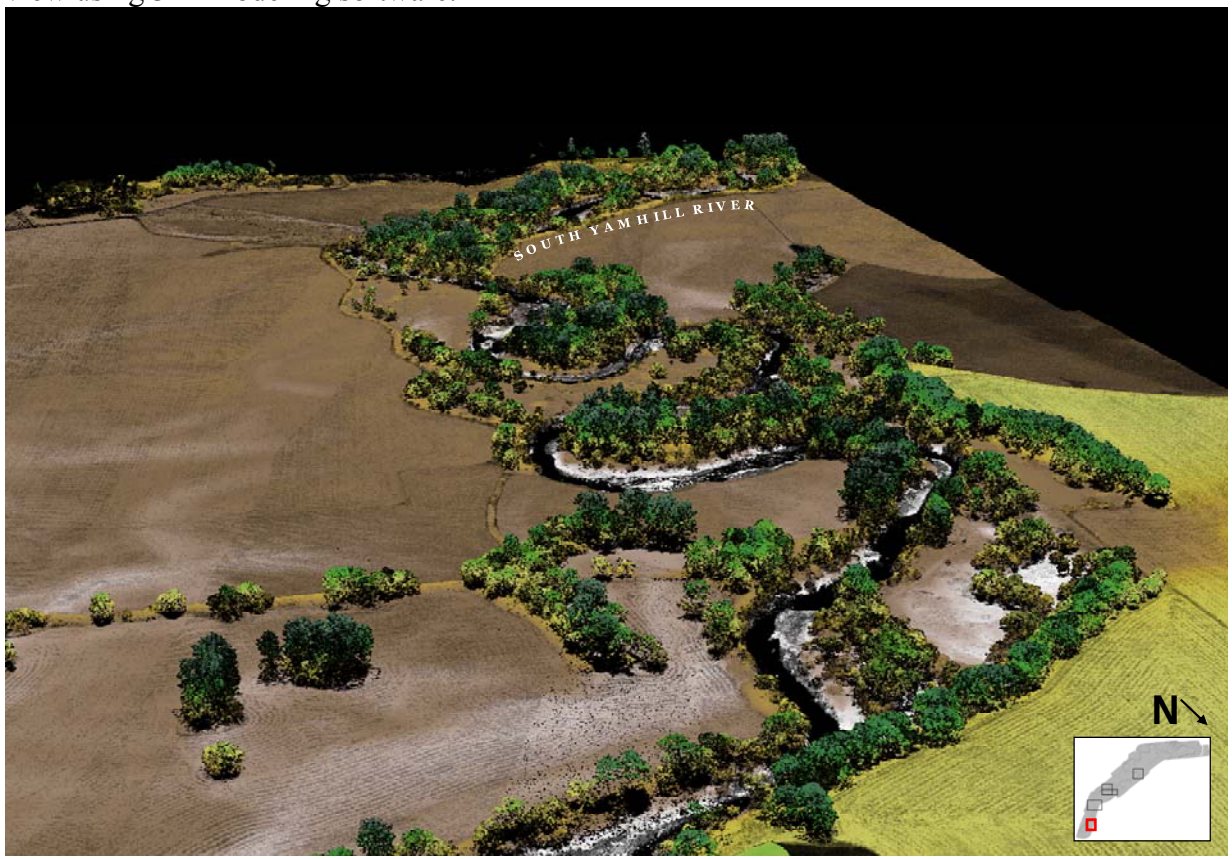

Figure 13. **0.5-meter** resolution bare ground surface, in upper portion of study area. Shown in oblique view using 3-D modeling software.

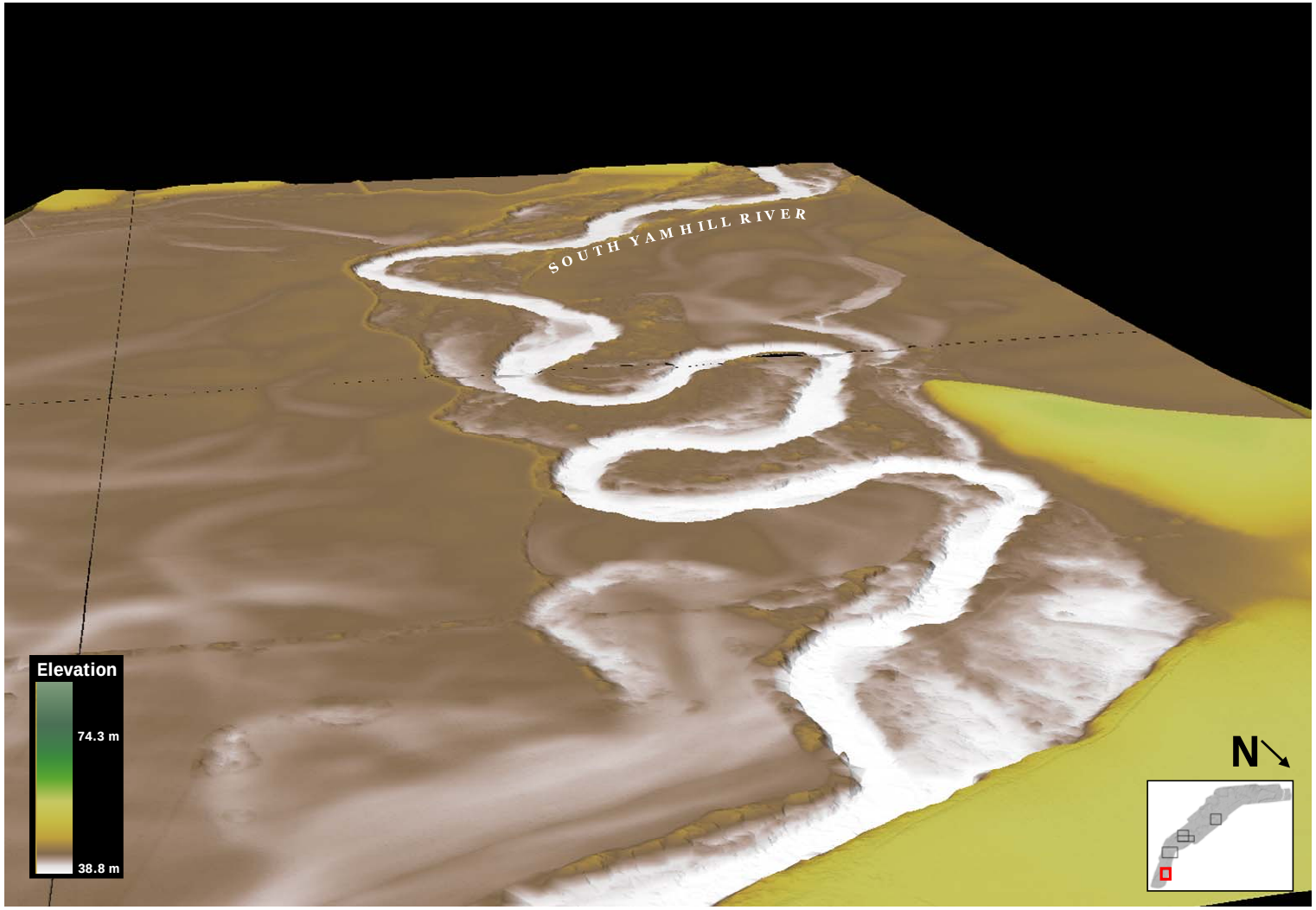

Figure 14. Point cloud of all points with intensity values, at confluence of Deer Creek (bins 21-26). Shown in oblique view using 3-D modeling software.

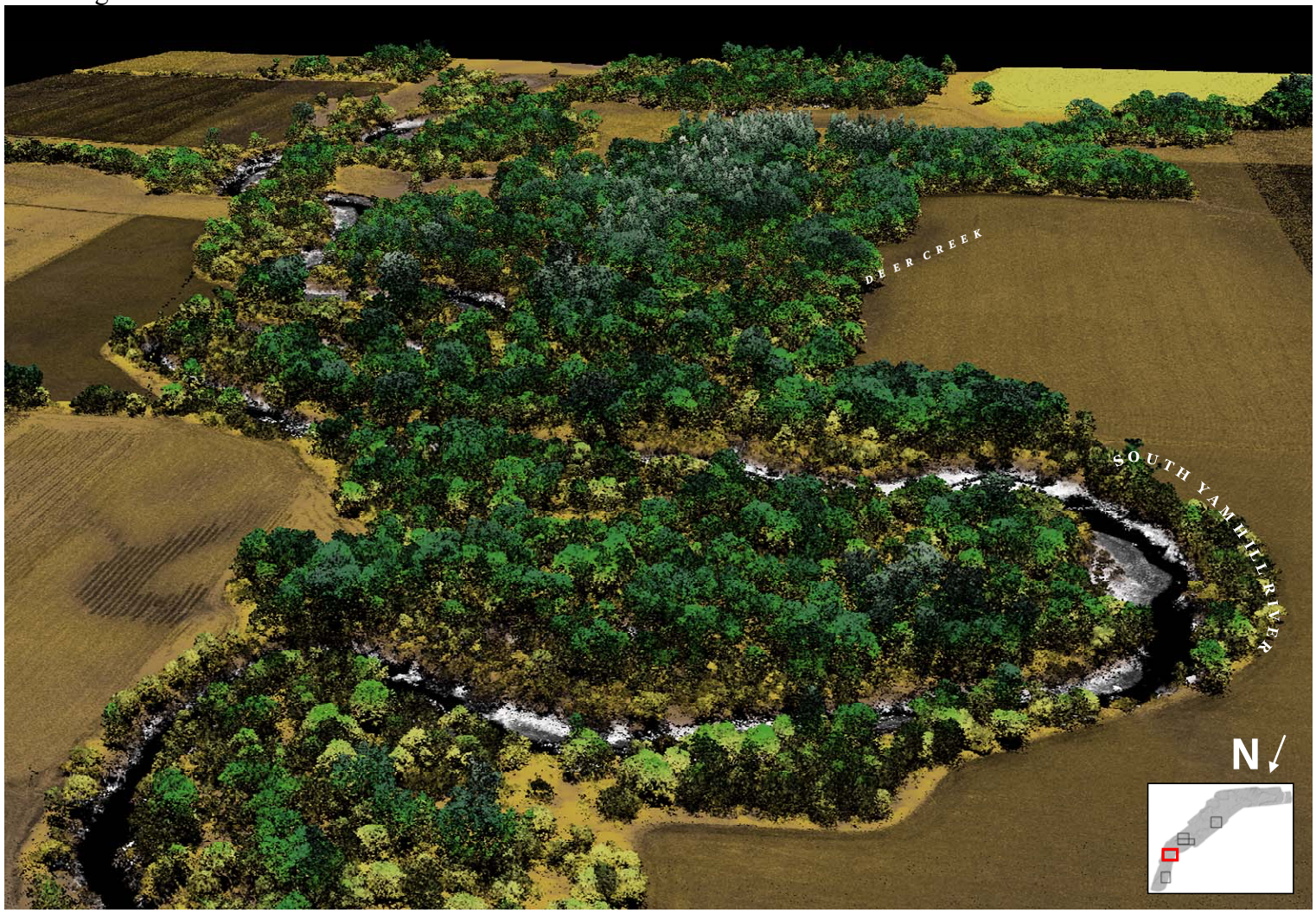

Figure 15. **0.5-meter** resolution bare ground surface, at confluence of Deer Creek (bins 21-26). Shown in oblique view using 3-D modeling software.

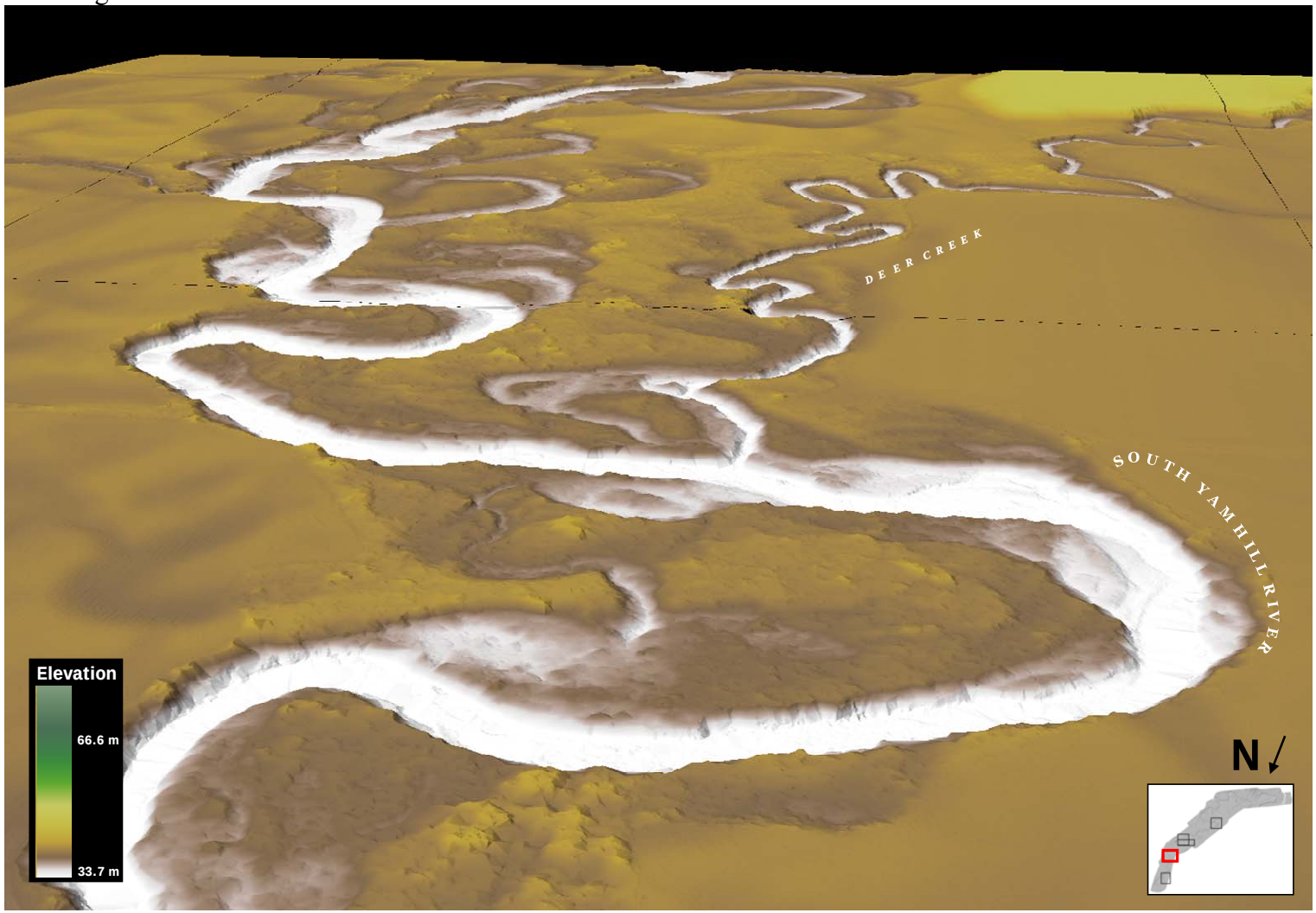

Figure 16. Point cloud of all points with intensity values, at confluence of Salt Creek (bins 38-40). Shown in oblique view using 3-D modeling software.

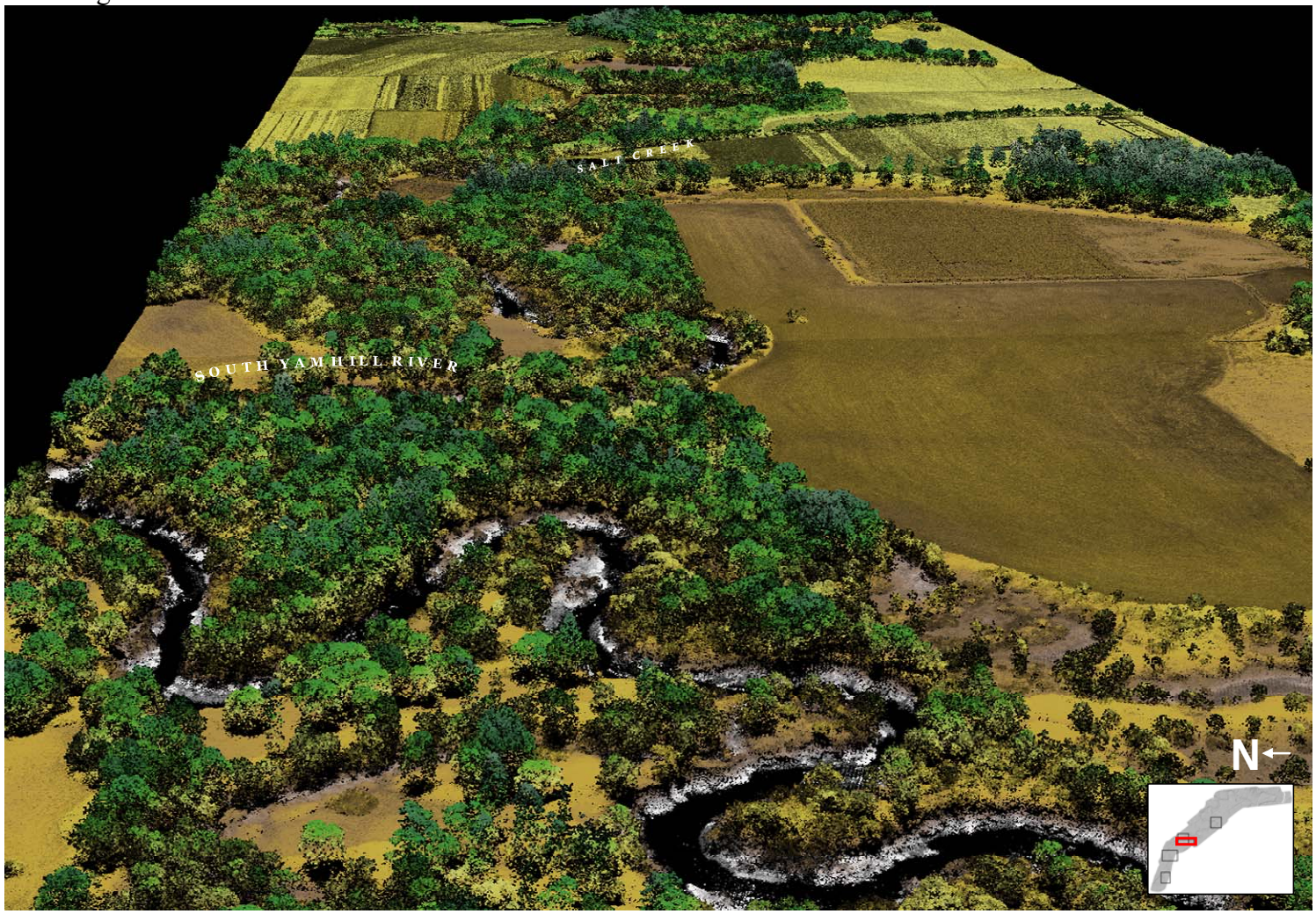

Figure 17. **0.5-meter** resolution bare ground surface, at confluence of Salt Creek (bins 38-40). Shown in oblique view using 3-D modeling software.

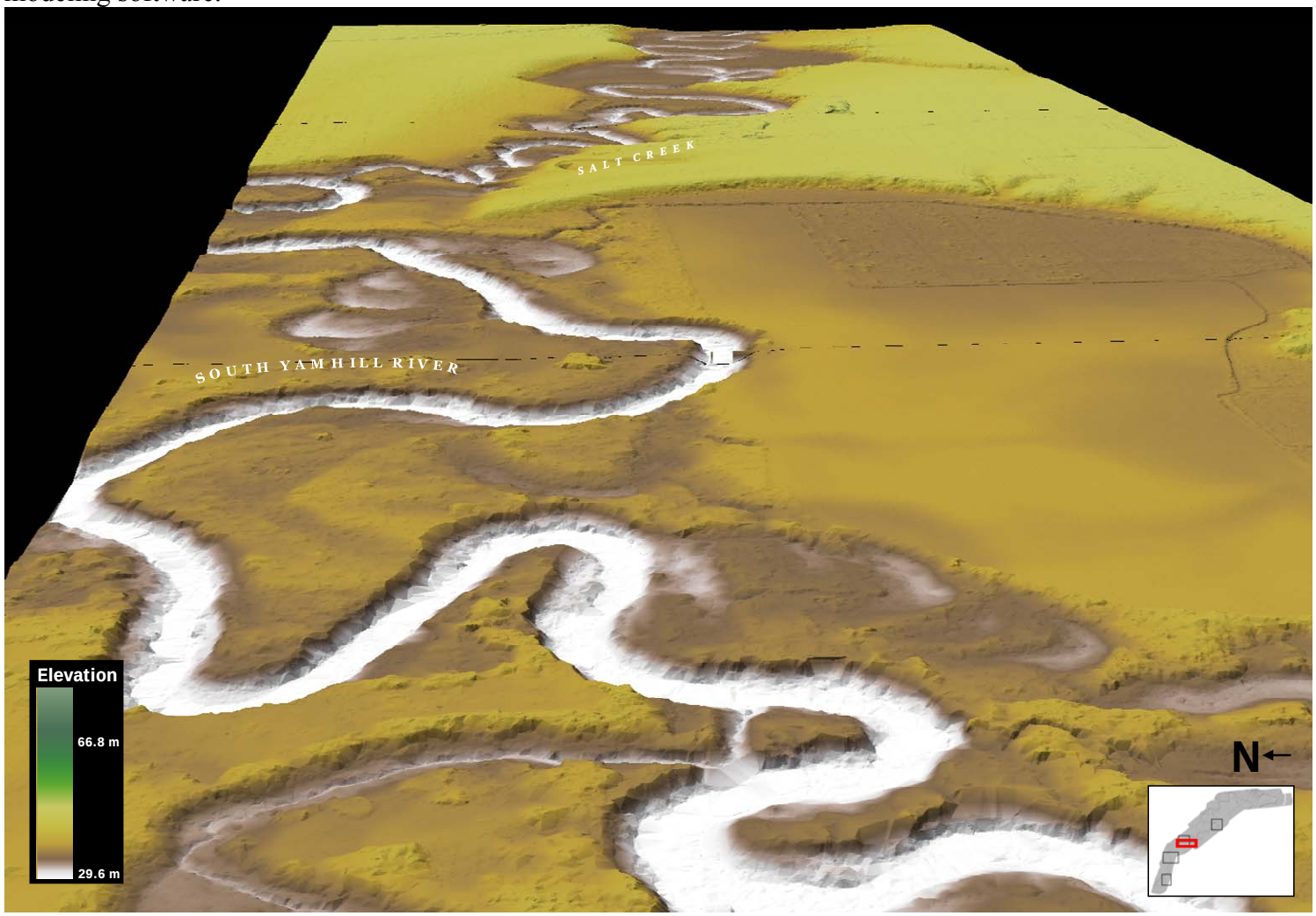

Figure 18. Point cloud of all points with intensity values, alternate view of confluence of Salt Creek (bins 38-39 & 44-45). Shown in oblique view using 3-D modeling software.

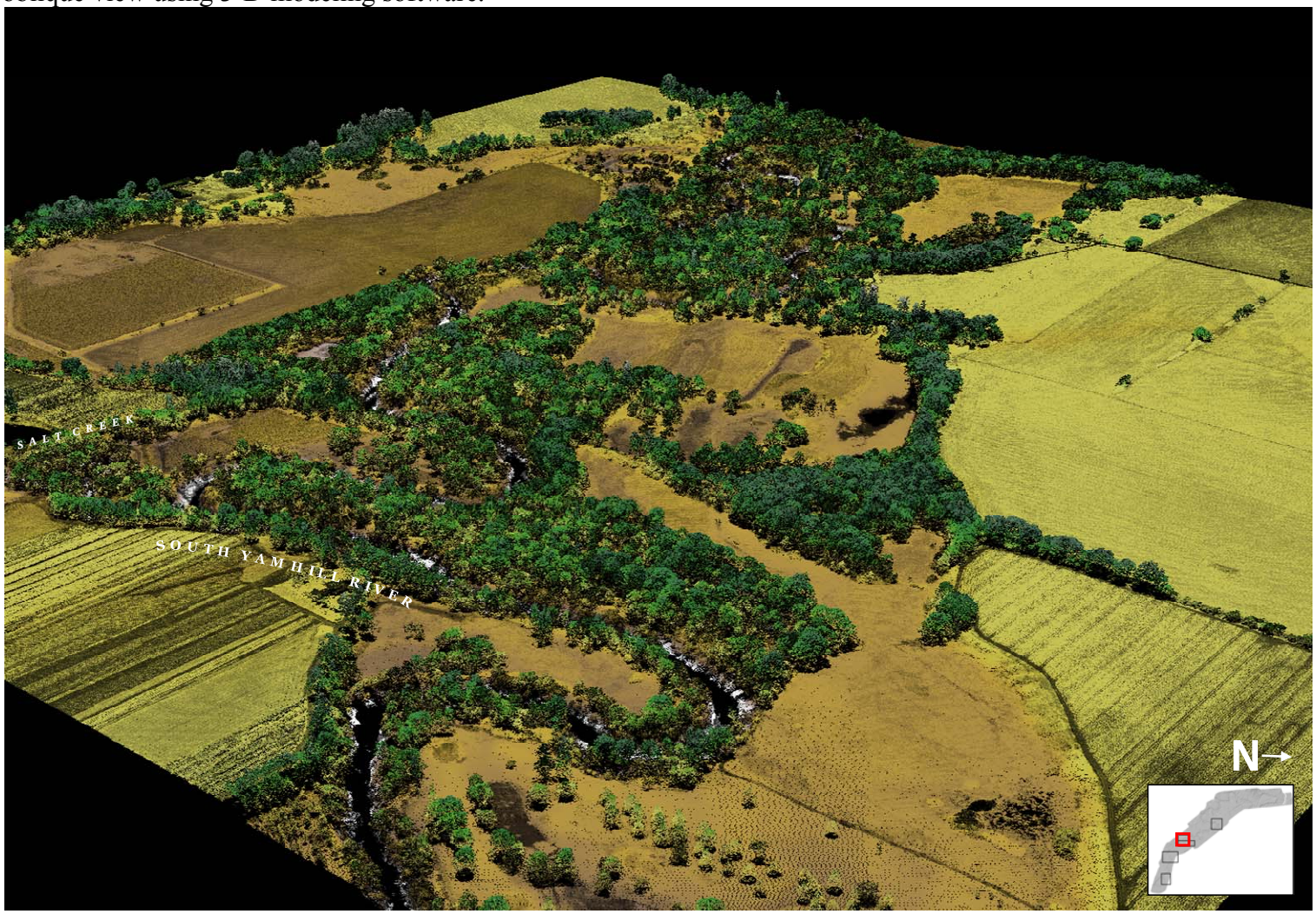

Figure 19. **0.5-meter** resolution bare ground surface, alternate view of confluence of Salt Creek (bins 38-39 & 44-45). Shown in oblique view using 3-D modeling software.

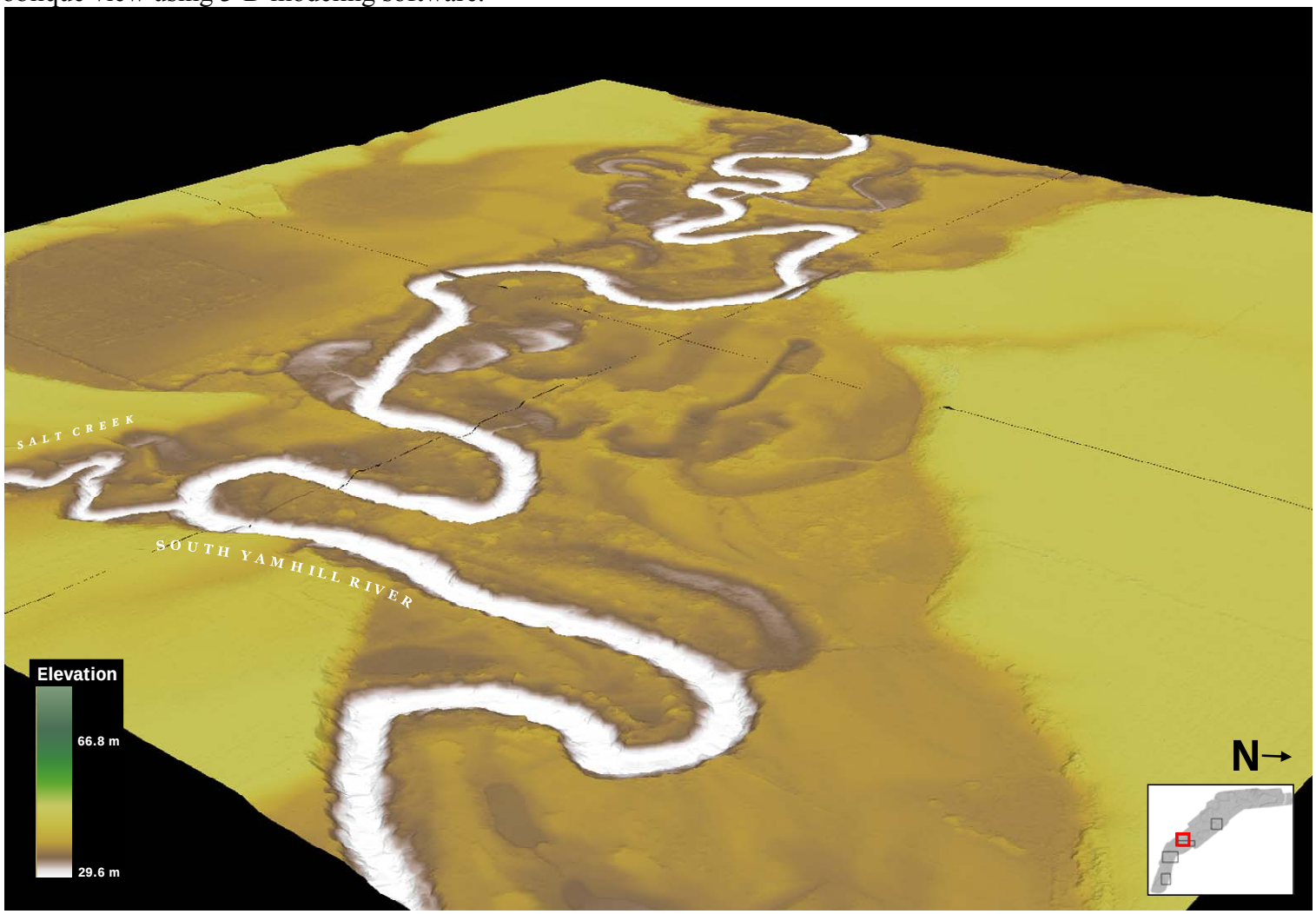

Figure 20. Point cloud of all points with intensity values, near McMinnville Airport (bins 62-63 & 69-70). Shown in oblique view using 3-D modeling software.

Figure 21. **0.5-meter** resolution bare ground surface, near McMinnville Airport (bins 62-63 & 69-70). Shown in oblique view using 3-D modeling software.

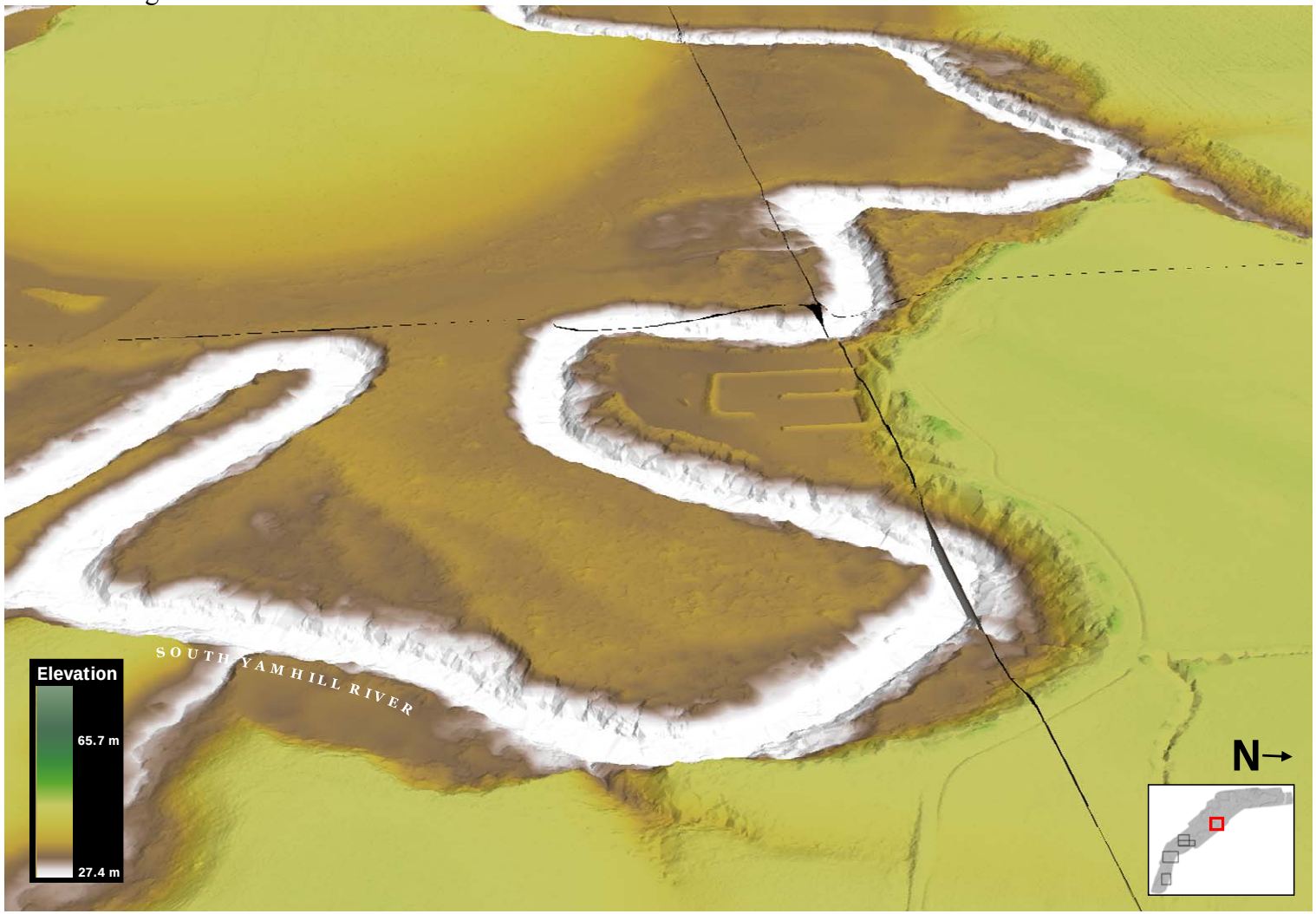

Citations

Andersen, H., R. McGaughey, W. Carson, S. Reutebuch, B. Mercer and J. Allan. 2003. A comparison of forest canopy models derived from LiDAR and INSAR data in a Pacific Northwest conifer forest. In: Proceedings of the ISPRS working group III/3 workshop '3-D reconstruction from airborne laserscanner and InSAR data'. Dresden, Germany.

Haugerud, R.A., and D. J. Harding. 2001. Some algorithms for virtual deforestation (VDF) of LiDAR topographic survey data. International Archives of Photogrammetry and Remote Sensing. XXXIV-3/W4, p. 211–217. http://www.isprs.org/commission3/annapolis/pdf/Haugerud.pdf. Las accessed February 15, 2006.

McGaughey, R. And W. Carson. 2003. Fusing LiDAR data, photographs, and other data using 2D and 3D visualization techniques. In: Proceedings of Terrain Data: Applications and Visualization – Making the Connection. Charleston, South Carolina: Bethesda, MD: American Society for Photogrammery and Remote Sensing. 16-24.

Soininen, A. 2004. TerraScan User's Guide. Terrasolid.

Watershed and Stream Delineation Tool. 2002. Texas A&M University. http://ceprofs.tamu.edu/folivera/GISTools/wsdt/home.htm. Last accessed February 15, 2006.